LWT - Food Science and Technology 222 (2025) 117635

Contents lists available at ScienceDirect

LWT

journal homepage: www.elsevier.com/locate/lwt

Monitoring salting kinetics of pork loin using magnetic resonance imaging (MRI) and time-domain nuclear magnetic resonance (TD-NMR)

Víctor Remiro [a,*], María Isabel Cambero [a], María Dolores Romero-de-Ávila [a], David Castejón [b], David Moreno-Molera [b], José Segura [a], María Encarnación Fernández-Valle [b]

[a] Department of Food Technology, Faculty of Veterinary Medicine, Complutense University of Madrid, Av. Puerta de Hierro s/n, 28040, Madrid, Spain
[b] Complutense Bioimaging Center (BIOMAC), Complutense University of Madrid, Paseo Juan XXIII, 1, 28040, Madrid, Spain

ARTICLE INFO

Keywords:
Salting kinetics
NaCl diffusion
Pork
MRI
TD-NMR

ABSTRACT

Magnetic resonance imaging (MRI) and time-domain nuclear magnetic resonance (TD-NMR) have been used as tools to monitor the salting process in pork loin. For this purpose, the longitudinal (T_1) and transverse (T_2) relaxation times, as well as the apparent diffusion coefficient (ADC), have been employed. To observe the changes occurring in meat pieces during the salting process and to obtain prediction models of the salt (NaCl) and water contents, the potential of each of these parameters has been evaluated. Surface models have been obtained that allow the observation of variations in T_1, T_2, and ADC MRI values related to salt diffusion and water loss during the salting process. Additionally, simple regression models have been established to determine the NaCl and water contents at any time during the process based on T_1 and T_2 values MRI values. On the other hand, to determine the NaCl content of the meat from the TD-NMR study, similar regression models were obtained with the mono-exponential analysis of T_1 and T_2 values. Additionally, the multi-exponential analysis of both T_1 and T_2 has provided insight into the effect of salt intake on the proton populations inside the meat. Thus, it is concluded that MRI and TD-NMR are highly suitable non-destructive techniques for the salt content determination and the monitoring of the salting process in the meat industry.

1. Introduction

In 2023, world meat production increased by 1.5% up to 371 Mt and, for the coming years, an annual 0.1% increase has been estimated in global meat consumption (FAO, 2024). Meat consists of long muscle fibers surrounded by layers of connective tissue and interspersed with adipose tissue, making it one of the most complex food matrices (Aguilera, 2019).

Non-destructive or minimally invasive technologies are widely used for the characterization and processing monitoring of food matrices. Sampling can depreciate the piece value thus making these methods essential in food processing plants, especially in the meat industry (Ali & Hashim, 2022). Traditional methods are time-consuming, and often destructive and subject to human error. Hence, several methodologies in meat and meat products (dry-cured ham, meat models …), such as ultrasound, X-rays, nuclear magnetic resonance (NMR) or infrared spectroscopy, are still under continuous study (Sánchez et al., 2022).

Recent studies in different food matrices define NMR as an interesting technology in the quality control of culinary oils (Castejón et al., 2017), in the determination of fish composition (Castejón et al., 2010), in the evaluation of the effect of irradiation on cheeses (Escudero et al., 2019) or in the determination of the quality of fruits and vegetables (Srivastava et al., 2018). Focusing on meat and meat products, Segura et al. (2023) described the application of NMR to game meat, and Castejón et al. (2015) and García-García, Herrera, et al. (2019) to the metabolomic analysis of meat exudates. The latter suggested the possibility that, by modifying the probe and the sampling procedure, the analyses could be carried out from the container itself.

"Within NMR, alternatives can be used for food analysis, among which are Magnetic Resonance Imaging (MRI) and time domain NMR (TD-NMR) relaxometry. Both techniques make it possible to determine non-invasively the content, mobility and distribution of water, as well as to analyze structural changes (Ezeanaka et al., 2019; Kuijpers et al., 2024). Both are suitable to study foodstuffs, as sample pretreatment is

* Corresponding author.
E-mail addresses: vremiro@ucm.es (V. Remiro), icambero@ucm.es (M.I. Cambero), mdavilah@ucm.es (M.D. Romero-de-Ávila), dcastejon@ucm.es (D. Castejón), davimo10@ucm.es (D. Moreno-Molera), josesegu@ucm.es (J. Segura), evalle@ucm.es (M.E. Fernández-Valle).

https://doi.org/10.1016/j.lwt.2025.117635
Received 27 November 2024; Received in revised form 23 January 2025; Accepted 9 March 2025
Available online 10 March 2025

not required (Sobolev et al., 2022). A great advantage of MRI and TD-NMR relaxometry is that they allow repeated measurements of several individual samples at consecutive times making it possible to monitor both microscopic and macroscopic changes in structure (Musse et al., 2009). MRI can be used to acquire morphological two-dimensional or three-dimensional images of interior of biological samples, providing spatial information of sample tissues, as the MRI signal depends on physical characteristics such as proton density, relaxation times, temperature, diffusion coefficient, etc. Quantitative MRI (qMRI) allows to quantify different morphological characteristics, as areas, volumes, etc., and to calculate spatially-resolved several NMR parameters, such as longitudinal (T_1) and transversal (T_2) relaxation times, proton density or apparent diffusion coefficient (ADC) (Mariette et al., 2012), providing complementary information relating to the composition and dynamics of the molecules that form the investigated tissues (Sobolev et al., 2022). On the other hand, TD-NMR also allows the quantification of relaxation times. Most TD-NMR relaxometers, as they are not equipped with gradients in the three spatial directions, get the information in a non-spatially-resolved manner, that is, of the whole sample. The higher signal to noise ratio and temporal resolution of this approach, compare with the great majority of qMRI studies, permit multi-exponential fitting of the TD-NMR data, and therefore getting the multi-component information of the relaxation curves and obtaining more information about sample microstructure. Most TD-NMR equipment operates at low magnetic field strength, which increases the accuracy of T_2 relaxation times because of the lower magnetic susceptibility effects. Using higher magnetic field strengths, as those used in MRI scanners, reduces the sensitivity of T_1 to molecular interactions (Musse et al., 2009).

Specifically, the potential of MRI to observe the internal structure and distribution of diverse types of tissues in meat matrices has also been described, thus being able to detect the presence of internal defects in hams (Remiro et al., 2024). Furthermore, the incorporation of NMR into production lines has also been described through rapid sequences (Melado Herreros et al., 2013, pp. 9–12). These results open the possibility of developing NMR for use in production lines in the future.

Salting is one of the most relevant stages in the manufacturing process of some meat products, which consists of using sodium chloride (NaCl) to increase the product shelf life by reducing microbial growth and providing specific sensory characteristics, such as a salty flavor or an appropriate texture (Pinton et al., 2021; Ríos-Mera et al., 2021). However, salt is one of the top dietary health concerns linked with diseases such as left ventricular hypertrophy, kidney disease, osteoporosis, asthma severity, stomach cancer, and hypertension, among others (He et al., 2020; Vinitha et al., 2022). For this reason, reducing salt content in products is one of the goals of the meat industry, thus making it imperative to know the salt content. In addition, official regulations exist on the salt content of cured products. For example, in dry-cured ham, salt content cannot exceed 15% on dry and defatted extract (European Commission, 1998) and, for pork loin, the average content is 4.7% (AESAN, 2010).

Salting kinetics of meat products, based on microstructural changes in the matrix due to the diffusion of NaCl, has been monitored with different non-destructive technologies such as ultrasounds (De Prados et al., 2017; Visy et al., 2021), X-ray absorptiometry (Fulladosa et al., 2015), near-infrared spectroscopy (Campos et al., 2020) or magnetic induction (Torres-Baix et al., 2024).

In this context, NMR emerges as a fast and non-invasive technology that does not use ionizing radiation. NMR parameters such as T_1 and T_2, and ADC have been used to evaluate the water content decrease or salt concentration increase in fish (Andreetta-Gorelkina et al., 2016; Liang et al., 2021). For salt diffusion monitoring, one of the alternatives offered by MRI is ^{23}Na-MRI. However, to fully assess the effect of salting on muscle structure, a relaxometry study is required (Clerjon & Bonny, 2017).

Generally, NMR has had the disadvantage of being an expensive technique and, therefore, difficult to implement in production lines. However, the appearance of economical low-field equipment and even benchtop relaxometry equipment in recent years enhances the possibility of using this technique in production lines. With this study, using pork loin as a model, the aim was to expand knowledge about the use of high field and low field NMR for the salting process monitoring in meat pieces. This comparison could provide information about the possibility of using low magnetic field equipment, which has great potential for industrial use.

2. Material and methods

2.1. Meat sampling

In order to obtain representative pieces, four fresh pork loins (*Longissimus thoracis et lumborum*, weight 4 ± 0.5 kg), from Large White × Landrace × Duroc gilts slaughtered at 100–120 kg live weight, were randomly acquired from a local abattoir of a leading and highly productive meat industry 48 h *post-mortem*. A portion of the medial zone (0.8–1.2 kg), corresponding to the *L. lumborum*, of each loin was selected for the study.

2.2. Salting

The pork loin portions were wrapped laterally with two layers of low-density polyethylene (LDPE) film for food use (Albal, Cofresco Ibérica, Madrid, Spain) leaving uncovered both the upper part (corresponding to the area closer to the skin) and the lower part (corresponding to the area closer to the body cavity). Each wrapped portion was placed in a plastic container and completely covered with salt (NaCl, 2.80 ± 0.46% moisture) so that the top and bottom surfaces were kept in direct contact with the salt (Fig. 1). The containers were kept closed and at 8 ± 2 °C until analysis.

At each analysis time (0, 1, 3, 5, 7, 24, 48 h), wrapped pieces were carefully cleaned of salt and weighed. Then, one slice (1 ± 0.2 cm thickness) was cut from each loin for subsequent analysis by MRI, TD-NMR, and then this slice was divided into 3 cuts (1.5 cm thickness) corresponding to the areas in direct contact with the salt (upper and lower external areas) and to the central area (Fig. 1) to determine the NaCl content.

After each sampling, and for the studied period (0–48 h), the remaining piece was wrapped laterally with the plastic film and covered with salt to continue the salting process.

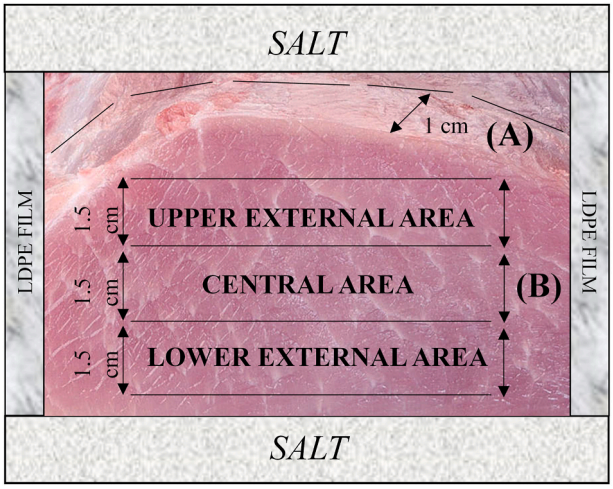

Fig. 1. Salting model: (A) Cutting slices to monitor the salting process at different times (0–48 h); (B) Transverse cuts in the slice to determine the NaCl content at different levels.

2.3. Monitoring of the salting process

2.3.1. Physicochemical analysis

In fresh samples, before salting, the following determinations were carried out: the ash content gravimetrically after treatment of the samples at 500 °C during 12 h (AOAC, 2012), the water holding capacity (WHC, %) by compression (Kauffman, Eikelenboom, Van der Wal, Engel, & Zaar, 1986), the protein content (%) by the Kjeldahl method 928.08 (AOAC, 2012), fat content (%) by Soxhlet method 991.36 (AOAC, 1996), the pH by puncture using a Crison pH25+ (Hash, Loveland, USA) pH meter and the water activity (a_w) using an AquaLab 4 TE (Barcelona, Spain) hygrometer at 25 °C. In fresh samples and at different salting times, the following were determined: the salt content (NaCl, %) was measured by AOAC method 971.19 (AOAC, 2000), the dry matter (DM, %) and moisture content gravimetrically by drying the sample at 110 °C to constant weight (AOAC, 2006) and the weight loss (WL) by difference of the weight of the piece before and after a salting period (Equation (1)). Before weighing, the surface of the meat was carefully cleaned to remove the presence of salt.

$$WL_t(\%) = \frac{(W_{t-1} - W_t) \times 100}{W_{t-1}} \quad \text{(Eq. 1)}$$

where W = weight, t = sampling time.

Every analysis was conducted in triplicate.

2.3.2. Nuclear magnetic resonance

2.3.2.1. Magnetic resonance imaging (MRI). MRI experiments were performed on the whole loin slice using a Bruker Biospec 47/40 spectrometer (Bruker BioSpin, Ettlingen, Germany) operating a 4.7 T, equipped with a 12-cm gradient system, using a 7-cm volume radio-frequency (RF) coil and a constant temperature of 18 °C.

For the T_2 values measurement, a multi-echo Carr-Purcell-Meiboom-Gill (CPMG) spin-echo sequence was used. Sixty echoes with echo times (TE) varied from 7.8 to 468 ms were acquired. This TE interval was used to cover a wide range of T_2 and to ensure the complete fall of the echo train signal. The repetition time (TR) was maintained at 4464 ms. Other imaging parameters were field of view (FOV) = 10 × 5 cm^2; slice thickness = 1.5 mm; number of slices = 3; and matrix size = 256 × 128.

For T_1 calculation, a spin-echo sequence with variable TR was considered. A series of six spin-echo images was acquired with logarithmically spaced TR (105.6–5105.5 ms) and constant TE (9 ms). The geometrical imaging parameters used were the same as those for the T_2 calculation.

A series of spin-echo images was acquired at four diffusion weightings for the ADC values calculation. The diffusion gradient duration (δ) was 10 ms and the time between gradients (Δ) was 25 ms. The gradient strengths varied from 5 to 190 mT/m, so the b-factor varied from 20.92 to 5943.34 s/mm^2. The geometrical imaging parameters used were the same as those used for the T_2 calculation, except for the matrix size, which was set to 128x64.

T_1, T_2, and ADC values were calculated using ParaVision 3.1 (Bruker Biospin, Ettlingen, Germany). On the central slice of the three slices acquired, one region of interest (ROI) in each area of the sample (upper external area, central area, and lower external area) was defined (Fig. S1). The values of the MRI parameters, T_1, T_2, and ADC, were obtained for every ROI fitting the mean signal of the ROI according to the equations described by Herrero et al. (2009).

2.3.2.2. Time domain nuclear magnetic resonance (TD-NMR). TD-NMR experiments were performed using a Bruker minispec LF90II TD-NMR analyzer (Bruker BioSpin, Ettlingen, Germany) operating at 0.146 T (6.2336 MHz), using a 9-cm RF probehead and at a constant temperature of 36 °C. T_1 and T_2 measurements were acquired for the whole loin slice.

For the T_1 calculation, an inversion-recovery sequence with variable inversion time (TI) was selected. TI values varied from 5 ms to 2000 ms and 12 different TI values were acquired. The TR was set to 2 s and four scans were averaged for each TI.

For the T_2 measurements, a multi-echo CPMG sequence was used. The TE was set to 403.52 ms and 4096 echoes were acquired. The TR was set to 2 s and 16 scans were averaged.

Relaxation times calculations were performed using a software developed by our research team using Matlab R2022b (The Mathworks Inc., Natick (MA), USA). First, an averaged T_1 and T_2 values for each sample were obtained fitting the signal curves to monoexponential functions (Herrero et al., 2009). Then, T_1 and T_2 continuous distributions were obtained by deconvolution with an inverse Laplace transform (Bjarnason & Mitchell, 2010).

2.4. Statistical analysis

Statistical analysis was conducted with Statgraphics 19-X64 for Windows (Statistical Graphics Corporation, Rockville, MD, USA). The data were presented as mean ± standard deviation. Different simple regression models were obtained between different parameters (salting time, NaCl content, water content, weight loss, T_2 and T_1). These regressions were evaluated using Durbin-Watson statistical tests, at a 95% confidence level. The R^2, standard error (SE), root mean squared error (RMSE), *F*-value and *p*-value were considered. Surface models between NaCl content, salting time and MRI parameters were obtained by a regression analysis to estimate the response function as: $Y = B_0 + B_1X_1 + B_2X_2 + B_{11}X_1^2 + B_{22}X_2^2 + B_{12}X_1X_2$, where Y is the NaCl content value, β_0 is a constant and β_1, β_2, β_{11}, β_{22} and β_{12} are the coefficients estimated from regression. They represent the linear, quadratic and cross-product effects of X_1 (salting time) and X_2 (MRI parameter) on the response. The backward stepwise procedure was used to select variables in the multivariate model (Chatterjee & Hadi, 2015, pp. 299–334). *F*-test was used to assess the significance of the equation parameters for each response variable.

3. Results and discussion

3.1. Physicochemical characterization

pH values of the pork loins ranged between 5.54 and 5.70, which is the common range in these pieces (Jo et al., 2023), and a_w values were characteristic of fresh pork (0.992–0.994) (Aliño et al., 2009). In order to guarantee an optimal salting process and the homogeneity of the samples, the basic composition of the pork loins was determined (Table S1). Chemical composition was typical of lean portions, with a percentage of DM between 25.3% and 26.5%, which is similar to previous studies carried out on pork loin (Karamucki et al., 2013), protein ranged from 92.6% to 93.6% (Jo et al., 2023), ash from 4.15% to 4.80% (Jo et al., 2022), and fat ranged from 2.22% to 3.14% (Lee et al., 2016) (Table S1). Protein, fat and ash values were obtained in DM. The value of the WHC ranged between 42.4 and 43.0%, similar to that described in the literature (Alvarado et al., 2011). NaCl content in the fresh pieces ranged between 0.08 and 0.23% (de Prados et al., 2017). The results of the physicochemical analysis of the studied matrices are shown in Table S1.

3.2. Salting kinetics and weight loss

Different salting kinetics were detected for different areas (Fig. 1) of the loins (Fig. 2 and Table S2). The salting kinetics of the upper and lower external areas fitted logarithmic models, but the central area showed two different stages (Fig. S2). In the external areas (upper and lower), a rapid salt gain was observed during the first 7 h, after which the salt uptake slowed down and stabilized in these external areas. Several authors also described a logarithmic model, with a maximum

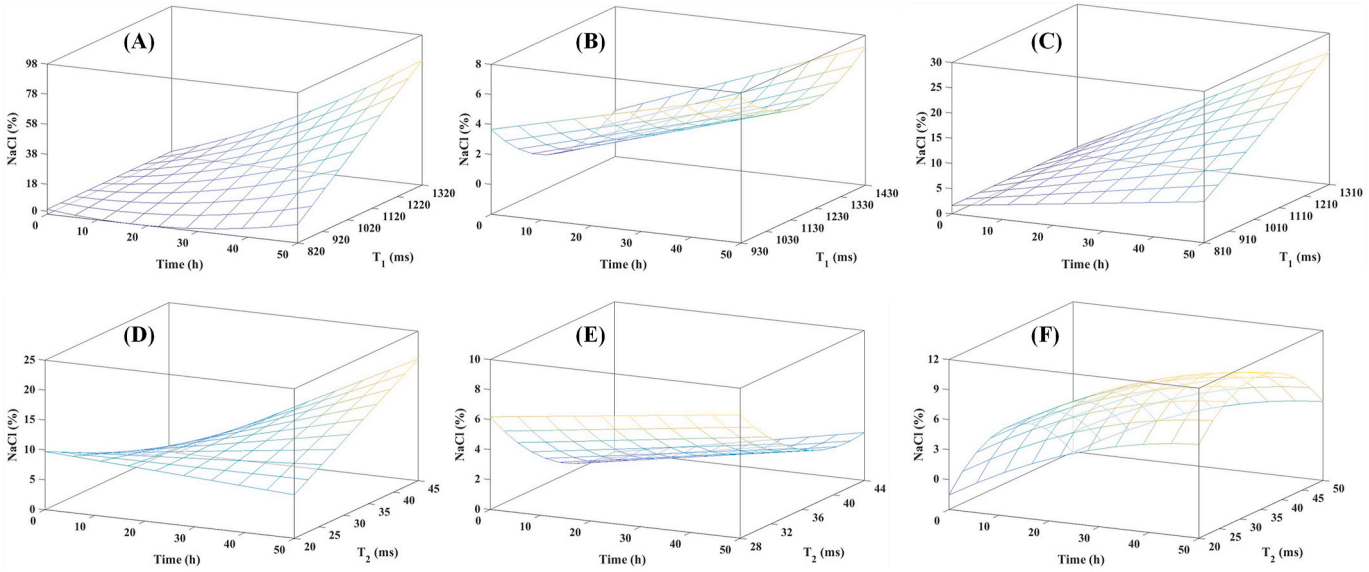

Fig. 2. Surface plots of regression models representing magnetic resonance imaging (MRI) parameters obtained at 4.7 T against salting time (h) and NaCl content (%). (A) Longitudinal relaxation time (T_1) upper external area; (B) T_1 central area; (C) T_1 lower external area; (D) Transversal relaxation time (T_2) upper external area; (E) T_2 central area; (F) T_2 lower external area. Regression model equations are shown in Table S2.

speed in a first stage, for pork salting using ultrasounds to force salt penetration (de Prados et al., 2017; Visy et al., 2021). This rapid salt uptake in the first hours of salting in the external areas was due to concentration differences and osmotic pressure. Furthermore, the higher salt concentration in the external areas subsequently hindered the salt uptake, explaining the reduction in the rate of salt uptake in the following hours (Sanches et al., 2023). In contrast to the external areas, the salting kinetics of the central area of the piece had two distinct stages. From 0 to 7 h of salting, the salt penetration rate was 0.06 g h^{-1} per 100 g for product, coinciding with the maximum rate of salt uptake in external areas. In this first period, the maximum salt content reached 0.44%. From 7 h up to 48 h, the penetration rate of the salt increased to 0.14 g h^{-1} per 100 g product, reaching a total salt content of 6.25%, compared to 8.89% in the lower external area and 10.09% in the upper external area (Fig. S2).

During the first hours of the salting process, there was a greater diffusion of water from the interior of the piece to the exterior, as well as a diffusion of salt from the exterior of the piece to the interior. This is because salt diffusion directly depends on water diffusion (Toldrá, 2004, pp. 27–62). Therefore, until the water content on the surface increases, the diffusion of salt into the interior is very slow. This is because it is necessary for the salt to dissolve in the water in order for it to diffuse (García-Gil et al., 2014). The osmotic gradient generated between the surface and the interior of the tissue during salting causes muscle contraction accompanied by water loss from the cells. Therefore, it can be stated that the direction of water flow during the salting process

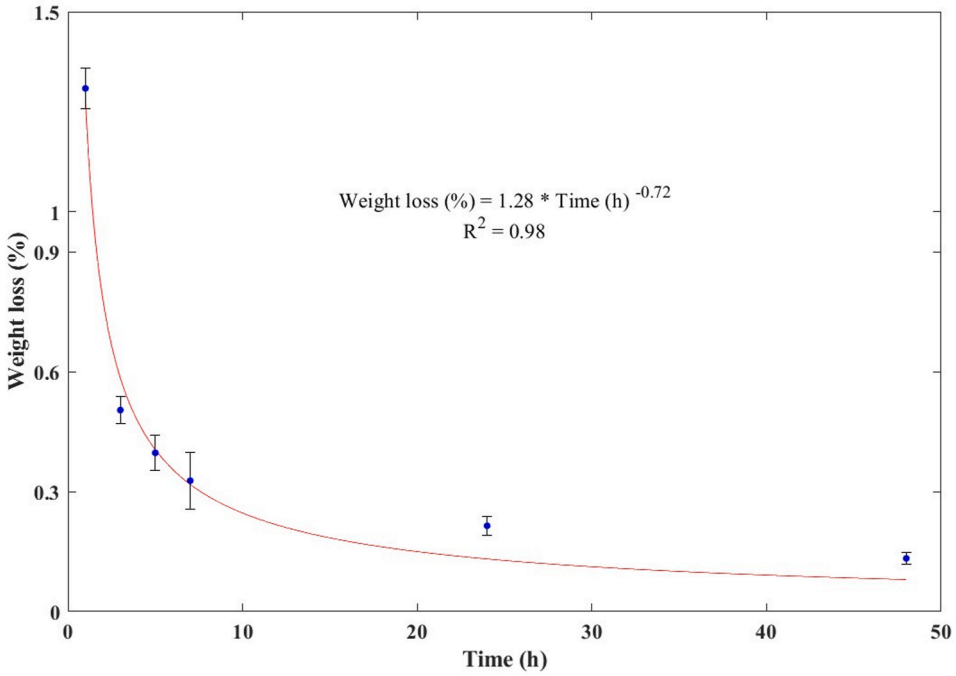

Fig. 3. Weight loss (WL) kinetic of pork loins during salting time. Mean and standard deviation (SD) of WL were considered. The equations and the R^2 are indicated.

directly depends on the salt concentration in the solution (Castro-Giraldez, Fito, & Fito, 2010; Yang et al., 2025). The main water population flowing during the salting stage is the freest water (Pearce et al., 2011).

On the other hand, the WL kinetics showed an inverse behavior to that of the salting kinetics in the external areas (Fig. 3). During the first hour of salting, the greatest drop in weight occurred, which was more than 1%. After 5 h of salting, WL ranged between 0.35 and 0.45%. This WL trend during the first hours of salting agrees with the results of Aliño et al. (2009) and de Prados et al. (2017) in pork loin. After this time, WL was reduced to below 0.25%, stabilizing the weight after 48 h. This greater WL during the first hours of salting may be caused by mass transfer mechanisms other than diffusion, such as the denaturation of surface proteins or the capillary forces of the salt in which the sample is placed (Aliño et al., 2009).

This stabilisation of WL and salt gain in the last hours of the salting process are closely related. Initially, the high salt concentration gradient between the outside and inside of the loins causes rapid salt diffusion and water loss. However, the rate of diffusion gradually decreases to equilibrium, at which point the net mass transfer flux is zero (Gómez-Salazar et al., 2015).

3.3. MRI relaxometry

T_1 and T_2 values decreased during the salting time at a higher rate in the external areas (upper and lower areas) than in the center of the piece (Fig. 2 and Table S2). This decrease in these values during the salting process was shown by other authors in dry-cured hams (Fantazzini et al., 2009; García-García, Fernández-Valle, et al., 2019). This slower decrease in the central area was due to the lower salt uptake and reduced dehydration, caused by the anaerobic conditions that occur in the interior of the piece. (García-García, Fernández-Valle, et al., 2019). One of the factors that affect to the decrease in the MRI parameters was the setting up of a water gradient from the inside to the surface of the loin pieces and from the surface to the environment, as a consequence of the flow of water that occurs by evaporation, osmotic dehydration and diffusion (García-García, Fernández-Valle, et al., 2019; Jurado et al., 2007). Related, it could also be associated with the compaction of the structure and physicochemical changes produced during the salting process (Richardson & Jones, 1987). These factors could explain the interaction (Table S2) between the salting time and T_1 and T_2 relaxation times ($p < 0.05$)

In addition to its decrease as salting time progresses, and directly related to it, Fig. 4 and Table S3 show the regression models between parameters T_1 and T_2 and the salt content. In both cases, the models fitted linear equations that are statistically significant ($R^2 = 0.89$ for T_1 and $R^2 = 0.90$ for T_2). Lower NaCl values corresponded to higher MRI parameter values.

In contrast to the evolution over time and salt content, Fig. 5 and Table S4 show the regression models between the moisture content of the loin pieces and the T_1 and T_2 parameters. Although the regressions fitted linear models that are statistically significant ($R^2 = 0.92$ for T_1 and $R^2 = 0.90$ for T_2), in this case, higher values of T_1 and T_2 corresponded to higher moisture content. As mentioned above, the T_1 and T_2 parameters were closely related to both salt and moisture content. Thus, the decrease in these values as salt uptake increases and water loss occurs is explained (García-García, Fernández-Valle, et al., 2019).

These results have great potential for the implementation of MRI in production lines of the meat industry. Through models similar to those obtained in this work, and adapted to the working conditions of each plant, the salt content, and also the water content, of a lean meat piece could be predicted at any time using only the T_1 and T_2 parameters. Thus, optimal quality can be ensured, meeting the desired requirements of the final product.

In the same way as with T_1 and T_2, the evolution of ADC values has also been monitored through regression models as salting time progresses, and thus, with salt uptake (Fig. 6 and Table S5). In the upper and lower external areas, the decrease in ADC values was faster than in the central area, since it was associated, among other factors, with the evolution of osmotic pressure gradients (Sanches et al., 2023). However, in the centre of the piece, the water movement and salt penetration depends on changes in the upper and lower external areas (García-Gil et al., 2014). The regression models obtained for the three areas studied were statistically significant ($R^2 = 0.92$ for upper external area, $R^2 = 0.96$ for central area and $R^2 = 0.89$ for lower external area). In the same way as occurred with T_1 and T_2 relaxation times, and for the reasons previously mentioned, a significant interaction ($p < 0.05$) was obtained between the ADC parameter and the salting time (Table S5).

Thus, ADC is a parameter that can also be used to monitor the salting process in pork loin, due to the close relationship between salt uptake and water movement within the piece.

3.4. Analysis by low field TD-NMR

As previously described, low-field NMR equipment is more economical and offers more possibilities for integration into production lines in the food industry. Therefore, after carrying out the study by high magnetic field MRI, the analysis was conducted on the same samples using TD-NMR at low field, to justify that this same analysis can be carried out at low field, in equipment much more adaptable to production lines.

Similar results to those obtained by MRI were obtained when the monoexponential adjustment of the TD-NMR T_1 and T_2 was made (Fig. 7 and Table S6). Once again, higher NaCl values were associated with lower T_1 and T_2 values. The linear regressions obtained, once more, were statistically significant ($R^2 = 0.90$ for T_1 and $R^2 = 0.82$ for T_2), indicating that low-field magnetic relaxometry equipment could also be used to determine the NaCl content of meat pieces through T_1 and T_2 values.

In addition to corroborating the results obtained previously with the monoexponential analysis of T_1 and T_2, a multiexponential study of both parameters was also carried out to observe the evolution of different proton populations in meat pieces during the salting process (Fig. 8). Regarding T_1, two populations were detected during the entire process. T_{1b} (with relaxation times of 35–45 ms), which could be associated with protons from water strongly bound to the myofibrils and T_{11} (with relaxation times ranging between 300 and 400 ms) which was associated with free water protons. These signals were also seen by Fantazzini et al. (2009) in their study of monitoring the salting process of Parma dry-cured ham, although the values were different due to the difference in the magnetic field of the spectrometer. The signal corresponding to T_{1b} remained stable throughout the salting time, which indicates that this population was not modified by the salt uptake and the loss of water from the sample throughout the process. For its part, signal T_{11} showed a displacement towards lower relaxation times in the last hours of salting than the beginning of the process. This displacement was associated, among other factors, with the loss of the water with lower degree of binding. The salt uptake in the piece caused a change in the charge of the myofibrillar protein, leading to increased contraction of the piece and greater WHC. (Richardson & Jones, 1987).

As for the T_2 multiexponential analysis, several populations were observed (Fig. 8). During the 48 h of salting, three populations were always present, which indicated that the relaxation behaviour in meat samples of these characteristics cannot be explained by intra/extracellular compartmentalisation of water (Bertram et al., 2001). T_{2b1} appears at 0–5 ms relaxation times, as Wu et al. (2006) shows in a study of pork. This population, which remained constant until 24 h salting but disappearing afterwards, would be a signal derived from what other authors have explained as T_{2b}, which corresponded to protons that are strongly bound to macromolecules, with a high degree of association with the matrix (García-García, Cambero, et al., 2019; Mcdonnell et al., 2013). In our case, this T_{2b} signal appeared divided into the

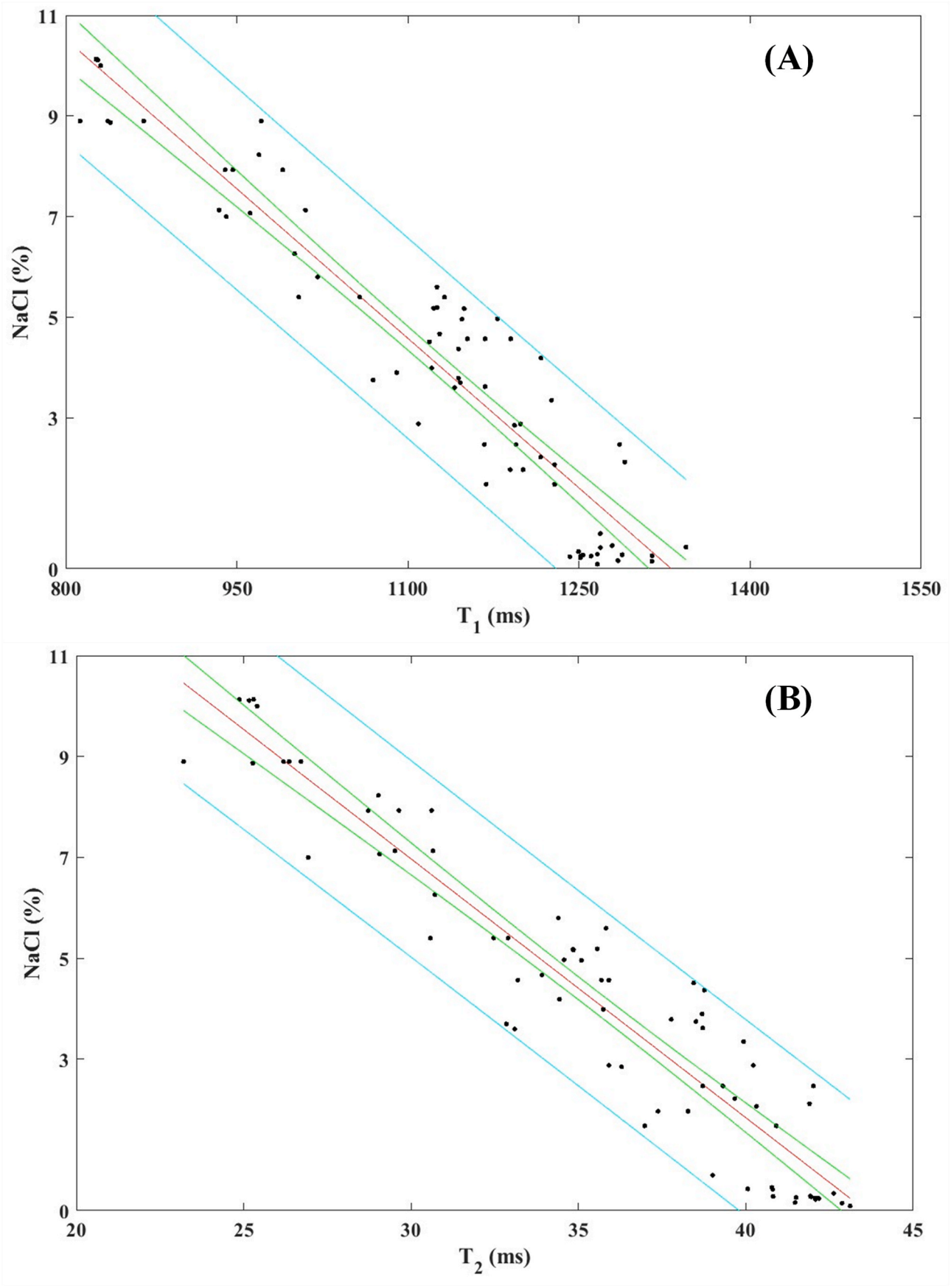

Fig. 4. Regression models between NaCl content (%) and magnetic resonance imaging (MRI) parameters obtained at 4.7 T. (A) Longitudinal relaxation time (T_1); (B) Transversal relaxation time (T_2). Regression model equations are shown in Table S3.

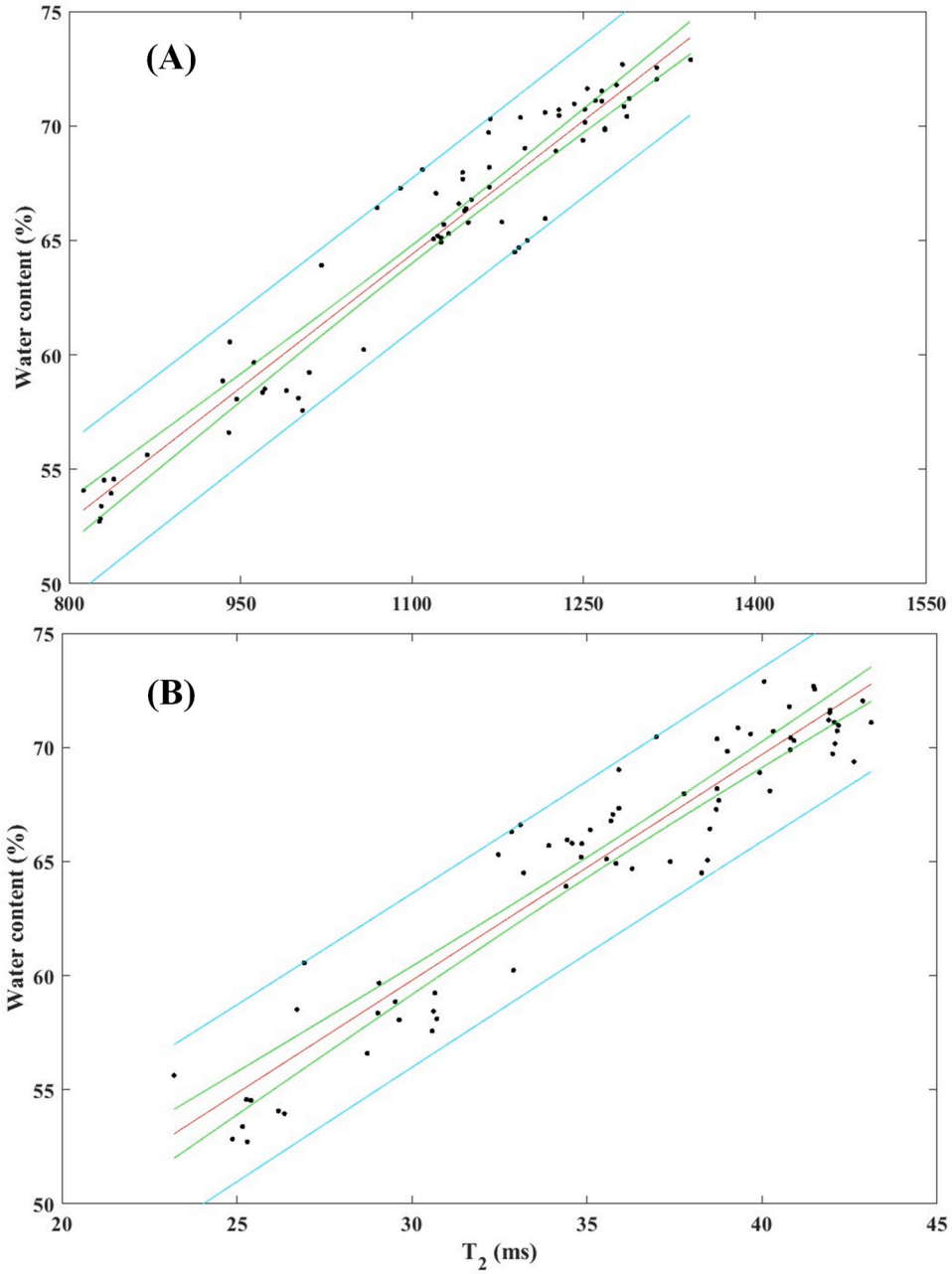

Fig. 5. Regression models between water content (%) and magnetic resonance imaging (MRI) parameters obtained at 4.7 T. (A) Longitudinal relaxation time (T_1); (B) Transversal relaxation time (T_2). Regression model equations are shown in Table S4.

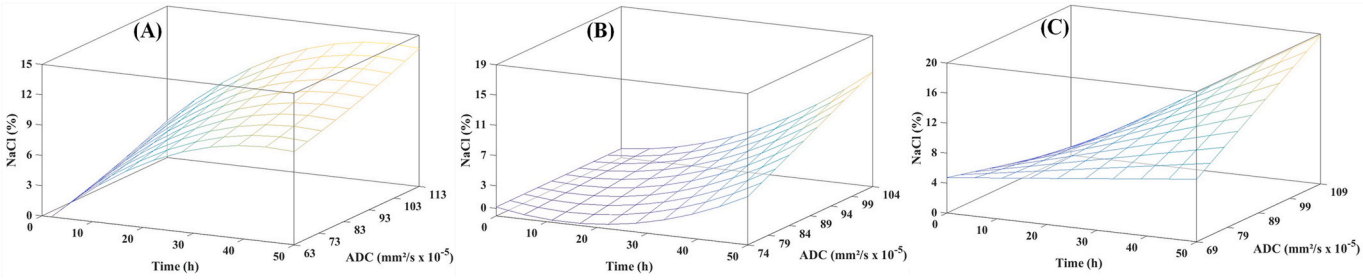

Fig. 6. Surface plots of regression models representing apparent diffusion coefficient (ADC) magnetic resonance imaging (MRI) parameter obtained at 4.7 T against salting time (h) and NaCl content (%). (A) ADC upper external area; (B) ADC central area; (C) ADC lower external area. Regression model equations are shown in Table S5.

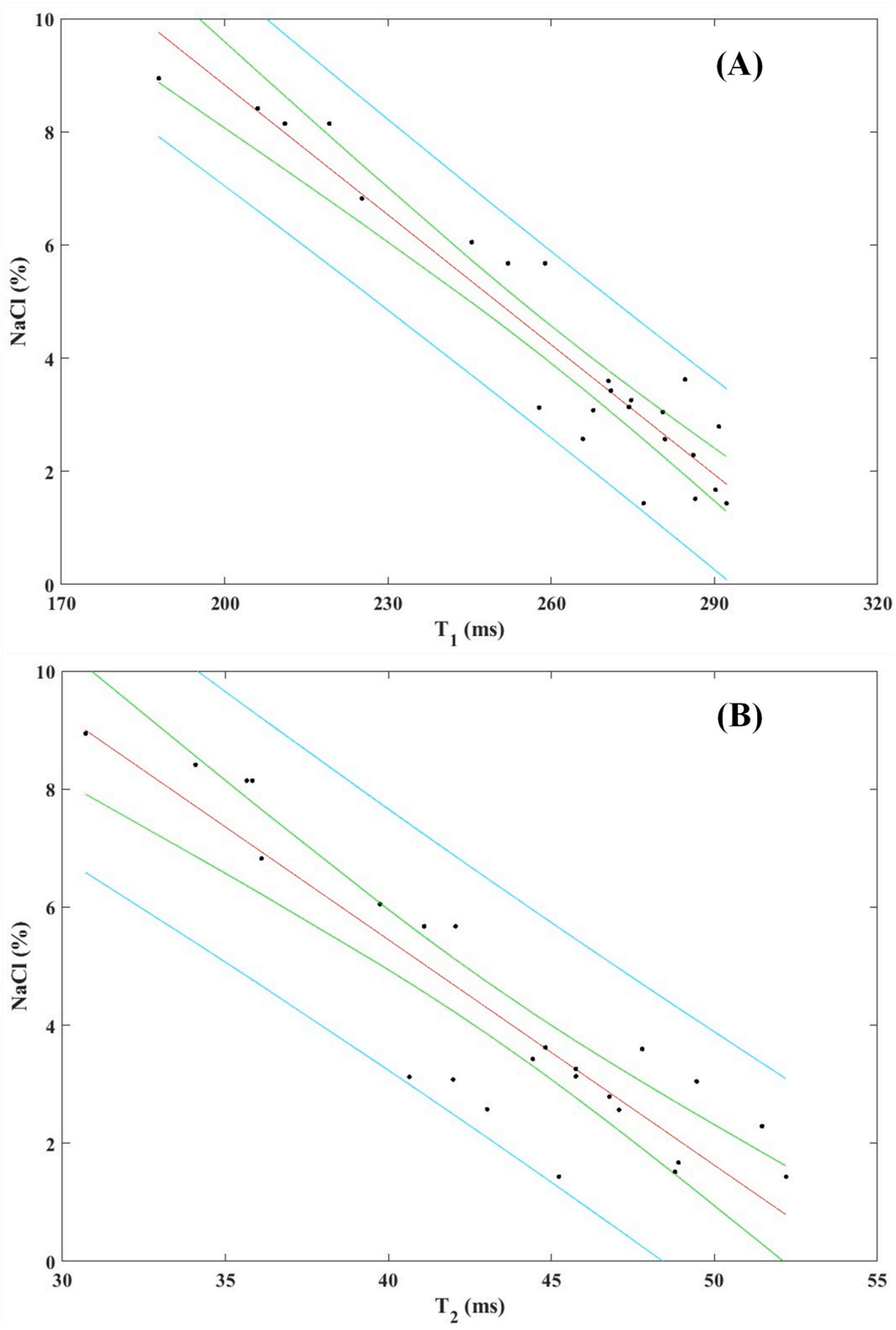

Fig. 7. Regression models between NaCl content (%) and time domain nuclear magnetic resonance (TD-NMR) monoexponential parameters obtained at 0.15 T. (A) Longitudinal relaxation time (T_1); (B) Transversal relaxation time (T_2). Regression model equations are shown in Table S6.

aforementioned T_{2b1} and a second T_{2b2} signal that appeared close to 10 ms relaxation times. In the same way that occurs with T_{2b1}, this signal moved to lower relaxation times in the last hours of the salting process. The other population that appeared throughout the study was T_{21}, which was the predominant signal with a relaxation time close to 40 ms. This population was related to the protons that are located within highly organized structures and corresponded to the water retained by the three-dimensional network of myofibrillar proteins in the space between the thick and thin filaments (Cònsolo et al., 2024; García-García, Cambero, et al., 2019; Mcdonnell et al., 2013). After 24 h of salting, a signal

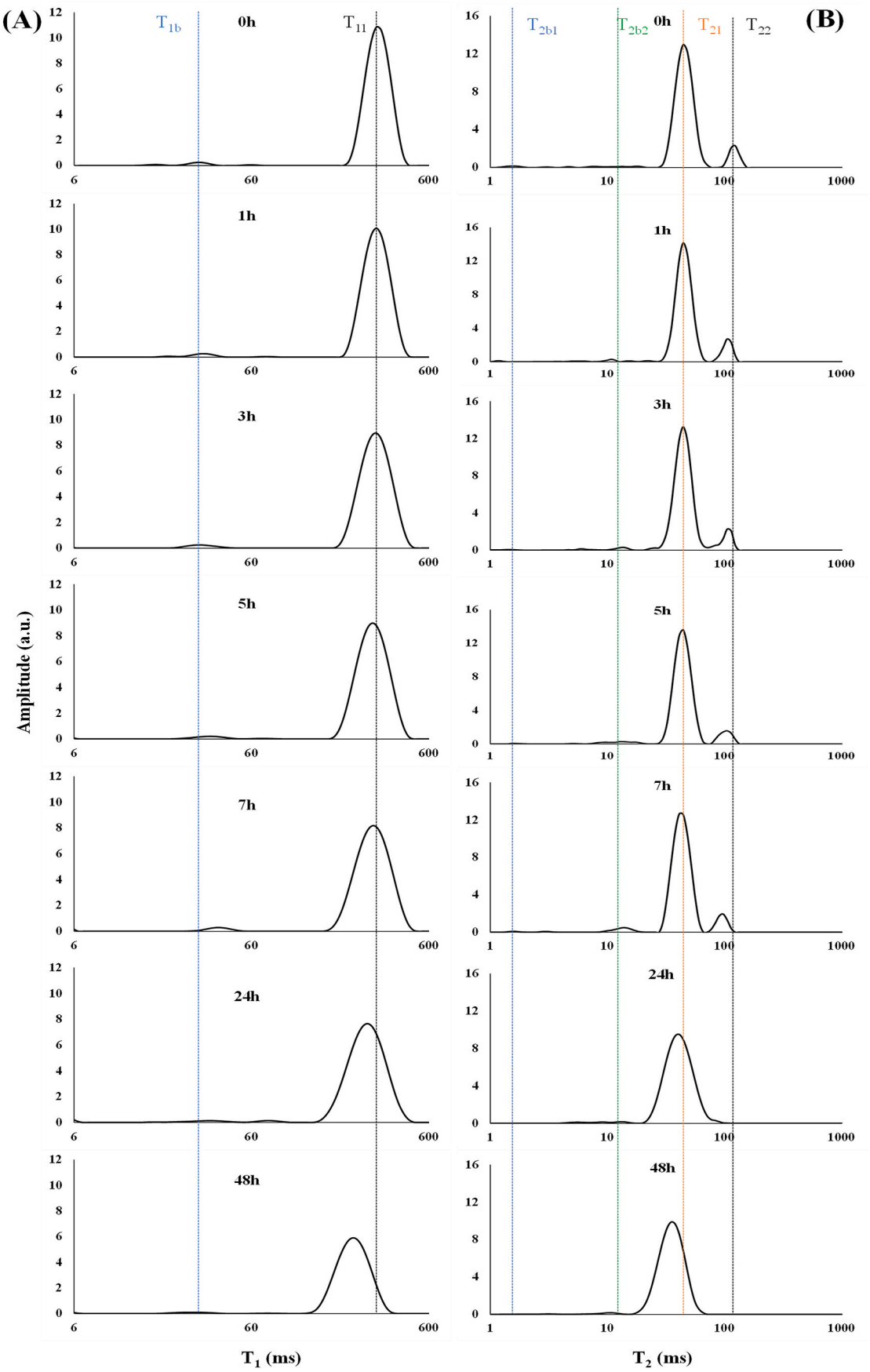

Fig. 8. Multiexponential spectra of time domain nuclear magnetic resonance (TD-NMR) parameters obtained at 0.15 T during the salting process of pork loins. (A) Longitudinal relaxation time (T_1); (B) Transversal relaxation time (T_2).

shift to lower relaxation times was detected. However, during the first 7 h of salting, a fourth population (T_{22}) appeared, with a relaxation time of 100 ms, which corresponded to extra-myofibrillar water containing the sarcoplasmic protein fraction and weakly retained between fibers (Bertram et al., 2001; Cônsolo et al., 2024; García-García, Cambero, et al., 2019; Mcdonnell et al., 2013). This water was the most labile and therefore the first to be lost when the salt began to enter, which would explain the displacement of this signal at lower relaxation times and its disappearance after 24 h of salting.

At very high salt concentrations, the elevated surface tension of water intensifies the competition between proteins and salt ions for hydration. This process causes the salt ions to remove the critical layer of water molecules from the protein surface, eventually resulting in the denaturation of the protein (Sinha & Khare, 2014). This protein denaturation causes a restriction of water mobility, resulting in shorter relaxation times (Gudjónsdóttir, Arason, & Rustad, 2011).

After the multiexponential T_2 analysis, it can be stated that during the salting of loin pieces, the signal from the free water disappeared, and the predominant water signal decreased. Meanwhile, the signals corresponding to more tightly bound water remained constant throughout the entire process.

With this study, an effort was made to provide the meat industry with a non-destructive and non-invasive alternative to the official method for determining the salt content of pork loin easily and quickly. This work is a first step for the future implementation of NMR in production lines. For this reason, more studies are needed to complete all the information necessary to be able to develop and implement this methodology in the industry.

4. Conclusions

The salting process of meat pieces can be monitored through MRI and TD-NMR as non-destructive and non-invasive techniques.

Salting kinetics of the pork loins fitted a logarithmic model in the external areas, while two distinct stages were observed in the centre of the piece, with the highest salt gain in the last hours of the process.

A decrease in NMR parameter values (relaxation times T_1 and T_2, and apparent diffusion coefficient) was observed throughout the salting process as a consequence of salt gain and water loss.

Prediction models can be used in the meat industry for the estimation of NaCl and water content at any point during the salting process of meat products, using NMR parameters (T_1, T_2, ADC).

Salt uptake and water movement during the salting process can be monitored through multiexponential analysis of NMR relaxation times (T_1 and T_2).

Finally, the results obtained in this work could permit us to conclude that the use of low magnetic field and low cost equipment allows the implementation of NMR relaxometry in the meat industry for monitoring and controlling the salting process, as well as for the rapid estimation of salt content.

CRediT authorship contribution statement

Víctor Remiro: Writing – review & editing, Writing – original draft, Supervision, Software, Methodology, Investigation, Formal analysis, Data curation, Conceptualization. **María Isabel Cambero:** Writing – review & editing, Supervision, Project administration, Methodology, Investigation, Funding acquisition, Formal analysis, Data curation, Conceptualization. **María Dolores Romero-de-Ávila:** Writing – review & editing, Writing – original draft, Supervision, Project administration, Methodology, Investigation, Funding acquisition, Formal analysis, Data curation, Conceptualization. **David Castejón:** Writing – review & editing, Writing – original draft, Supervision. **David Moreno-Molera:** Supervision, Methodology. **José Segura:** Writing – review & editing, Writing – original draft, Supervision. **María Encarnación Fernández-Valle:** Writing – review & editing, Supervision, Software, Methodology, Investigation, Formal analysis, Data curation, Conceptualization.

Funding sources

The present work received financial support from Project PID2019-107542RB-C22: Nuclear magnetic resonance (NMR) methodologies as automation and control tools in the meat sector, funded by the Spanish Secretary of State of Research, Development and Innovation within the Ministry of Economy and Competitiveness. V. Remiro was awarded a predoctoral fellowship from the Community of Madrid.

Declaration of competing interest

The authors declare that they have no known competing financial interests or personal relationships that could have appeared to influence the work reported in this paper.

Acknowledgments

Thanks to the funding project PID2019-107542RB-C22: Metodologías de Resonancia Magnética Nuclear (RMN) como herramientas de automatización y control en el sector cárnico. To BioImaC (Bioimagen Complutense), one of the nodes of the ICTS ReDiB. To Bruker Española S. A. for fully providing the Bruker minispec LF90II (Bruker Biospin, Ettlingen, Germany) equipment, which was essential to this study, with no expectation of remuneration or return. To the predoctoral fellowship from the Community of Madrid.

Appendix A. Supplementary data

Supplementary data to this article can be found online at https://doi.org/10.1016/j.lwt.2025.117635.

Data availability

Data will be made available on request.

References

AESAN. (2010). Informe del Comité Científico de la Agencia Española de Seguridad Alimentaria y Nutrición (AESAN) en relación al efecto de la reducción de la sal en la seguridad microbiológica de los productos cárnicos curados. *Agencia Española de Seguridad Alimentaria y Nutrición, 13*(010), 64–68.

Aguilera, J. M. (2019). The food matrix: Implications in processing, nutrition and health. *Critical Reviews in Food Science and Nutrition, 59*(22), 3612–3629. https://doi.org/10.1080/10408398.2018.1502743

Ali, M. M., & Hashim, N. (2022). Non-destructive methods for detection of food quality. In R. Bhat (Ed.), *Future foods* (pp. 645–667). Academic Press.

Aliño, M., Grau, R., Baigts, D., & Barat, J. M. (2009). Influence of sodium replacement on the salting kinetics of pork loin. *Journal of Food Engineering, 95*(4), 551–557. https://doi.org/10.1016/j.jfoodeng.2009.06.016

Alvarado, J. G. G., Lara, R. A. G., García, J. L. A., Pozos, R. L., Rivera, E. D. J. R., & Rojo, A. D. A. (2011). Efecto del método de insensibilización sobre los parámetros más importantes que influyen en el sacrificio y calidad de la carne de cerdo. *Nacameh, 5*(2), 40–55.

Andreetta-Gorelkina, I. V., Gorelkin, I. V., & Rustad, T. (2016). Determination of apparent diffusion coefficient in balls made from haddock mince during brining. *Journal of Food Engineering, 175*, 8–14. https://doi.org/10.1016/j.jfoodeng.2015.11.016

AOAC. (1996). Official method 991.36. Fat (crude) in meat and meat products. Soxhlet extraction method. *Official methods of analysis* (16th ed.). Washington D. C., EEUU: AOAC International.

AOAC. (2000). Official method 971.19-1971. Salt (sodium chloride) in food. Volumetric method. *Official methods of analysis* (17th ed.). Washington D. C., EEUU: AOAC International.

AOAC. (2006). Official method 950.46. *Moisture in Meat. Official methods of analysis* (18th ed.). Washington D. C., EEUU: AOAC International.

AOAC. (2012). Official method 928.08. Protein in meat. Kjeldahl method. *Official methods of analysis* (19th ed.). Washington D. C., EEUU: AOAC International.

Bertram, H. C., Karlsson, A. H., Rasmussen, M., Pedersen, O. D., Dønstrup, S., & Andersen, H. J. (2001). Origin of multiexponential T 2 relaxation in muscle myowater. *Journal of Agricultural and Food Chemistry, 49*(6), 3092–3100. https://doi.org/10.1021/jf001402t

Bjarnason, T. A., & Mitchell, J. R. (2010). AnalyzeNNLS: Magnetic resonance multiexponential decay image analysis. *Journal of Magnetic Resonance, 206*(2), 200–204.

Campos, M. I., Debán, L., Antolín, G., & Pardo, R. (2020). Evaluation by NIRS technology of curing process of ham with low sodium content. *Meat Science, 163*. https://doi.org/10.1016/j.meatsci.2020.108075

Castejón, D., García-Segura, J. M., Escudero, R., Herrera, A., & Cambero, M. I. (2015). Metabolomics of meat exudate: Its potential to evaluate beef meat conservation and aging. *Analytica Chimica Acta, 901*, 1–11. https://doi.org/10.1016/j.aca.2015.08.032

Castejón, D., Herrera, A., Heras, Á., Cambero, M. I., & Mateos-Aparicio, I. (2017). Oil quality control of culinary oils subjected to deep-fat frying based on NMR and EPR spectroscopy. *Food Analytical Methods, 10*, 2467–2480. https://doi.org/10.1007/s12161-016-0778-x

Castejón, D., Villa, P., Calvo, M. M., Santa-María, G., Herráiz, M., & Herrera, A. (2010). ^{1}H-HRMAS NMR study of smoked Atlantic salmon (Salmo salar). *Magnetic Resonance in Chemistry, 48*(9), 693–703. https://doi.org/10.1002/mrc.2652

Castro-Giraldez, M., Fito, P. J., & Fito, P. (2010). Non-equilibrium thermodynamic approach to analyze the pork meat (Longissimus dorsi) salting process. *Journal of Food Engineering, 99*(1), 24–30. https://doi.org/10.1016/j.jfoodeng.2010.01.023

Chatterjee, S., & Hadi, A. S. (2015). *Variable selection procedures*. New Jersey: John Wiley & Sons. Regression analysis by example.

Clerjon, S., & Bonny, J. M. (2017). NMR imaging of meat. In G. Webb (Ed.), *Modern magnetic resonance* (pp. 1609–1628). Cham, S: Springer International Publishing. https://doi.org/10.1007/978-3-319-28275-6_131-1.

Cônsolo, N. R., de Paula, A. P., Rezende-de-Souza, J. H., Herreira, V. L., Gôngora, A. L. S., Colnago, L. A., et al. (2024). Assessment of water relaxometry of meat under different ageing processes using time domain nuclear magnetic resonance relaxometry. *Food Research International.* , Article 114566. https://doi.org/10.1016/j.foodres.2024.114566

De Prados, M., García-Pérez, J. V., & Benedito, J. (2017). Non-invasive ultrasonic technology for continuous monitoring of pork loin and ham dry salting. *Meat Science, 128*, 8–14. https://doi.org/10.1016/j.meatsci.2017.01.009

Escudero, R., Segura, J., Velasco, R., Valhondo, M., Romero de Ávila, M. D., García-García, A. B., et al. (2019). Electron spin resonance (ESR) spectroscopy study of cheese treated with accelerated electrons. *Food Chemistry, 276*, 315–321. https://doi.org/10.1016/j.foodchem.2018.09.101

Ezeanaka, M. C., Nsor-Atindana, J., & Zhang, M. (2019). Online low-field nuclear magnetic resonance (LF-NMR) and magnetic resonance imaging (MRI) for food quality optimization in food processing. *Food and Bioprocess Technology, 12*(9), 1435–1451. https://doi.org/10.1007/s11947-019-02296-w

Fantazzini, P., Gombia, M., Schembri, P., Simoncini, N., & Virgili, R. (2009). Use of magnetic resonance imaging for monitoring Parma dry-cured ham processing. *Meat Science, 82*(2), 219–227. https://doi.org/10.1016/j.meatsci.2009.01.014

FAO. (2024). Meat market review: Overview of global meat market in 2023. Rome. https://openknowledge.fao.org/bitstreams/ae4eb1ec-613d-478c-8361-c9bdba1df559/download. (Accessed 22 July 2024).

Fulladosa, E., Muñoz, I., Serra, X., Arnau, J., & Gou, P. (2015). X-ray absorptiometry for non-destructive monitoring of the salt uptake in bone-in raw hams during salting. *Food Control, 47*, 37–42. https://doi.org/10.1016/j.foodcont.2014.06.023

García-García, A. B., Cambero, M. I., Castejón, D., Escudero, R., & Fernández-Valle, M. E. (2019). Dry cured-ham microestructure: A T_2 NMR relaxometry, SEM and uniaxial tensile test combined study. *Food Structure, 19*, Article 100104. https://doi.org/10.1016/j.foostr.2018.100104

García-García, A. B., Fernández-Valle, M. E., Castejón, D., Escudero, R., & Cambero, M. I. (2019). Use of MRI as a predictive tool for physicochemical and rheological features during cured ham manufacturing. *Meat Science, 148*, 171–180. https://doi.org/10.1016/j.meatsci.2018.10.015

García-García, A. B., Herrera, A., Fernández-Valle, M. E., Cambero, M. I., & Castejón, D. (2019a). Evaluation of E-beam irradiation and storage time in pork exudates using NMR metabolomics. *Food Research International, 120*, 553–559. https://doi.org/10.1016/j.foodres.2018.11.005

García-Gil, N., Muñoz, I., Santos-Garcés, E., Arnau, J., & Gou, P. (2014). Salt uptake and water loss in hams with different water contents at the lean surface and at different salting temperatures. *Meat Science, 96*(1), 65–72. https://doi.org/10.1016/j.meatsci.2013.06.012

Gómez-Salazar, J. A., Clemente-Polo, G., & Sanjuán-Pelliccer, N. (2015). Review of mathematical models to describe the food salting process. *Dyna, 82*(190), 23–30. https://doi.org/10.15446/dyna.v82n190.42016

Gudjónsdóttir, M., Arason, S., & Rustad, T. (2011). The effects of pre-salting methods on water distribution and protein denaturation of dry salted and rehydrated cod–A low-field NMR study. *Journal of Food Engineering, 104*(1), 23–29. https://doi.org/10.1016/j.jfoodeng.2010.11.022

He, F. J., Tan, M., Ma, Y., & MacGregor, G. A. (2020). Salt reduction to prevent hypertension and cardiovascular disease: JACC state-of-the-art review. *Journal of the American College of Cardiology, 75*(6), 632–647. https://doi.org/10.1016/j.jacc.2019.11.055

Herrero, A. M., de la Hoz, L., Ordóñez, J. A., Castejón, D., Romero de Ávila, M. D., & Cambero, M. I. (2009). Magnetic resonance imaging study of the cold-set gelation of meat systems containing plasma powder. *Food Research International, 42*(9), 1362–1372. https://doi.org/10.1016/j.foodres.2009.06.014

Jo, K., Lee, S., Jeong, H. G., Lee, D. H., Kim, H. B., Seol, K. H., et al. (2022). Prediction of cooking loss of pork belly using quality properties of pork loin. *Meat Science, 194* (108957). https://doi.org/10.1016/j.meatsci.2022.108957

Jo, K., Lee, S., Jeong, H. G., Lee, D. H., Yoon, S., Chung, Y., et al. (2023). Utilization of electrical conductivity to improve prediction accuracy of cooking loss of pork loin. *Food Science of Animal Resources, 43*(1), 113. https://doi.org/10.5851/kosfa.2022.e64

Jurado, Á., García, C., Timón, M. L., & Carrapiso, A. I. (2007). Effect of ripening time and rearing system on amino acid-related flavour compounds of Iberian ham. *Meat Science, 75*(4), 585–594. https://doi.org/10.1016/j.meatsci.2006.09.006

Karamucki, T., Jakubowska, M., Rybarczyk, A., & Gardzielewska, J. (2013). The influence of myoglobin on the colour of minced pork loin. *Meat Science, 94*(2), 234–238. https://doi.org/10.1016/j.meatsci.2013.01.014

Kauffman, R. G., Eikelenboom, G., Van der Wal, P. G., Engel, B., & Zaar, M. (1986). A comparison of methods to estimate water-holding capacity in post-rigor porcine muscle. *Meat Science, 18*(4), 307–322. https://doi.org/10.1016/0309-1740(86)90020-3

Kuijpers, S. A., Goudappel, G. J., Huppertz, T., van Duynhoven, J. P., & Terenzi, C. (2024). Quantification of phase separation in high moisture soy protein extrudates by NMR and MRI. *Food Research International, 197*, Article 115225. https://doi.org/10.1016/j.foodres.2024.115225

Lee, C. W., Lee, J. R., Kim, M. K., Jo, C., Lee, K. H., You, I., et al. (2016). Quality improvement of pork loin by dry aging. *Korean Journal for Food Science of Animal Resources, 36*(3), 369. https://doi.org/10.5851/kosfa.2016.36.3.369

Liang, Y., Xie, Y., Li, D., Luo, Y., & Hong, H. (2021). Dynamics of water mobility, salt diffusion and hardness changes in bighead carp fillets during low-salting. *Lebensmittel-Wissenschaft und -Technologie, 135*, Article 110033. https://doi.org/10.1016/j.lwt.2020.110033

Mariette, F., Collewet, G., Davenel, A., Lucas, T., & Musse, M. (2012). Quantitative MRI in food science & food engineering. *Encyclopedia of Magnetic Resonance, 1*, 205–214. https://doi.org/10.1002/9780470034590.emrstm1272

McDonnell, C. K., Allen, P., Duggan, E., Arimi, J. M., Casey, E., Duane, G., et al. (2013). The effect of salt and fibre direction on water dynamics, distribution and mobility in pork muscle: A low field NMR study. *Meat Science, 95*(1), 51–58. https://doi.org/10.1016/j.meatsci.2013.04.012

Melado Herreros, A., Fernández Valle, M. E., Hernandez Sanchez, N., Jiménez Ariza, H. T., Verlinden, B. E., Val, J., et al. (2013). On-line MRI sequences for the evaluation of apple internal quality. *InsideFood symposium*. April 2013, Leuven, Belgium.

Musse, M., Quellec, S., Cambert, M., Devaux, M. F., Lahaye, M., & Mariette, F. (2009). Monitoring the postharvest ripening of tomato fruit using quantitative MRI and NMR relaxometry. *Postharvest Biology and Technology, 53*(1–2), 22–35. https://doi.org/10.1016/j.postharvbio.2009.02.004

Official Journal of the European Communities. (1998). *Publication of an application for registration pursuant to the second subparagraph of Article 8(1) of Regulation (EEC) No. 2082/92 on certificates of specific character*. C 371, 1.12.

Pearce, K. L., Rosenvold, K., Andersen, H. J., & Hopkins, D. L. (2011). Water distribution and mobility in meat during the conversion of muscle to meat and ageing and the impacts on fresh meat quality attributes—a review. *Meat Science, 89*(2), 111–124. https://doi.org/10.1016/j.meatsci.2011.04.007

Pinton, M. B., dos Santos, B. A., Lorenzo, J. M., Cichoski, A. J., Boeira, C. P., & Campagnol, P. C. B. (2021). Green technologies as a strategy to reduce NaCl and phosphate in meat products: An overview. *Current Opinion in Food Science, 40*, 1–5. https://doi.org/10.1016/j.cofs.2020.03.011

Remiro, V., Cambero, M. I., García-Real, M. I., Romero de Ávila, M. D., Castejón, D., Santos, C., et al. (2024). Aplicación de la Imagen de Resonancia Magnética (IRM) al análisis morfológico no destructivo de piezas cárnicas. Una aproximación a la selección de perniles. *ITEA-Información Técnica Económica Agraria, 120*(3), 224–238. https://doi.org/10.12706/itea.2023.018

Richardson, R. I., & Jones, J. M. (1987). The effects of salt concentration and pH upon water-binding, water-holding and protein extractability of Turkey meat. *International Journal of Food Science and Technology, 22*(6), 683–692. https://doi.org/10.1111/j.1365-2621.1987.tb00537.x

Ríos-Mera, J. D., Selani, M. M., Patinho, I., Saldaña, E., & Contreras-Castillo, C. J. (2021). Modification of NaCl structure as a sodium reduction strategy in meat products: An overview. *Meat Science, 174*, Article 108417. https://doi.org/10.1016/j.meatsci.2020.108417

Sanches, M. A. R., Lapinskas, N. M., Barretto, T. L., da Silva-Barretto, A. C., & Telis-Romero, J. (2023). Improving salt diffusion by ultrasound application during wet salting of pork meat: A mathematical modeling approach. *Journal of Food Process Engineering, 46*(6), Article e14143. https://doi.org/10.1111/jfpe.14143

Sánchez, P. D. C., Arogancia, H. B. T., Boyles, K. M., Pontillo, A. J. B., & Ali, M. M. (2022). Emerging nondestructive techniques for the quality and safety evaluation of pork and beef: Recent advances, challenges, and future perspectives. *Applied Food Research, 2*(2), Article 100147. https://doi.org/10.1016/j.afres.2022.100147

Segura, J., Remiro, V., Romero-de-Ávila, M. D., Villa, P., Castejón, D., Santos, C., et al. (2023). Game meat and high-resolution magic angle spinning nuclear magnetic resonance spectroscopy: A traditional foodstuff versus a novel analysis technology. *Animal Frontiers, 13*(6), 56–61. https://doi.org/10.1093/af/vfad066

Sinha, R., & Khare, S. K. (2014). Protective role of salt in catalysis and maintaining structure of halophilic proteins against denaturation. *Frontiers in Microbiology, 5*, 165. https://doi.org/10.3389/fmicb.2014.00165

Sobolev, A. P., Ingallina, C., Spano, M., Di Matteo, G., & Mannina, L. (2022). NMR-based approaches in the study of foods. *Molecules, 27*(22), 7906. https://doi.org/10.3390/molecules27227906

Srivastava, R. K., Talluri, S., Beebi, S. K., & Rajesh Kumar, B. (2018). Magnetic resonance imaging for quality evaluation of fruits: A review. *Food Analytical Methods, 11*, 2943–2960. https://doi.org/10.1007/s12161-018-1262-6

Toldrá, F. (2004). Manufacturing of dry-cured ham. *Dry-cured meat products*. Food & Nutrition Press, INC.

Torres-Baix, E., Illana, A., Gou, P., Olmos, A., Arnau, J., & Fulladosa, E. (2024). Modelling of salt uptake for salt content standardization in dry-cured ham. *Meat Science, 214*, Article 109523. https://doi.org/10.1016/j.meatsci.2024.109523

Vinitha, K., Sethupathy, P., Moses, J. A., & Anandharamakrishnan, C. (2022). Conventional and emerging approaches for reducing dietary intake of salt. *Food Research International, 152*, Article 110933. https://doi.org/10.1016/j.foodres.2021.110933

Visy, A., Jónás, G., Szakos, D., Horváth-Mezőfi, Z., Hidas, K. I., Barkó, A., et al. (2021). Evaluation of ultrasound and microbubbles effect on pork meat during brining process. *Ultrasonics Sonochemistry, 75*, Article 105589. https://doi.org/10.1016/j.ultsonch.2021.105589

Wu, Z., Bertram, H. C., Kohler, A., Böcker, U., Ofstad, R., & Andersen, H. J. (2006). Influence of aging and salting on protein secondary structures and water distribution in uncooked and cooked pork. A combined FT-IR microspectroscopy and ^{1}H NMR relaxometry study. *Journal of Agricultural and Food Chemistry, 54*(22), 8589–8597. https://doi.org/10.1021/jf061576w

Yang, K., Wu, R., Khoder, R. M., Xiong, S., & Liu, R. (2025). Mathematical modelling the variation of sodium chloride (NaCl) diffusion behavior and quality of grass carp fillets during salting. *Journal of Food Engineering, 391*, Article 112439. https://doi.org/10.1016/j.jfoodeng.2024.112439